

4.1 Fourier Transform Infrared Spectroscopy

O. FAIX

4.1.1 Principles and Instrumental Techniques

4.1.1.1 Introduction

Since the early 1950s, IR spectroscopy has been a routine analytical tool for lignin chemists. In the past, spectra were recorded using the so-called dispersive technique, i.e., with grating-type or prism instruments. In the last decade, Fourier transform infrared (FTIR) spectrometers have become increasingly available for routine laboratory work.

4.1.1.2 Scope of FTIR Spectroscopic Applications

FTIR spectroscopy may be applied to good advantage in such specialized areas as micro analysis where high sensitivity is required, in the analysis of aqueous solutions or dark, solid state samples that require the use of special reflectance techniques, in investigations placing emphasis on quantitative evaluation, and in experiments where analysis time is a limiting factor, e.g., in process or quality control measurements.

4.1.1.3 Description of a Standard FTIR Instrument

In FTIR spectroscopy, an interference wave interacts with the sample in contrast to a dispersive instrument where the interacting energy assumes a well-defined wavelength range. The interference wave is produced in an interferometer (Fig. 4.1.1), the most common of which is the Michelson interferometer. A computer is used to control the interferometer, to collect and store data, and to perform the Fourier transformation. In addition, the computer performs post-spectroscopic operations such as spectral presentation, resolution enhancement, calibration, and calculation of correlation equations.

A collimated light beam from the IR source is directed to the Michelson interferometer where it is divided by the beam splitter. One half of the beam is reflected from a fixed mirror and the other half from a moving mirror. The two light beams recombine after returning from the mirrors and give rise to a reconstructed beam which is optically an interference wave. The interference light beam passes through the sample and is modified by its interaction with the

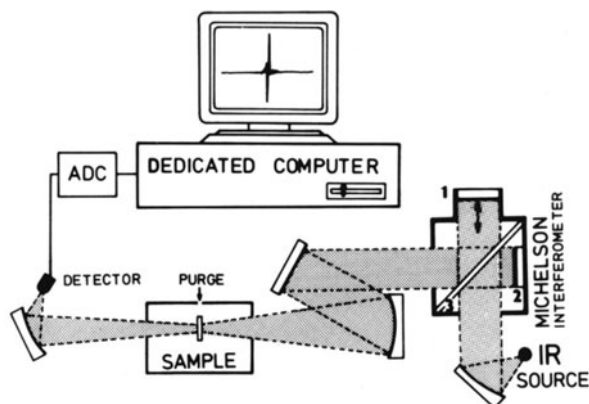


Fig. 4.1.1. Schematic diagram of a FTIR instrument: 1 moving mirror; 2 fixed mirror; 3 beam splitter made of KBr or CsI as supporter coated with a thin germanium layer. ADC analog-digital-converter

sample. Usually, a deuterated triglycine sulfate (DTGS) pyroelectric detector receives the modified light. The analog signals arriving at the detector are digitized by an analog-digital-converter (ADC) and stored in the computer. Laser technology is indispensable for good performance in this procedure. A laser beam undergoes the same change of optical path in the interferometer as the IR beam. Hence, it can serve as a reference for the position of the mirror during the scan. The laser beam also governs the collection of data points as a function of the movement of the mirror.

A complete IR spectrum can be reconstructed after only one cycle of mirror movement by use of the fast Fourier transform algorithm (Cooley and Tukey 1965). If time is not a limiting factor, additional scans are usually made. After each addition, an average interferogram is calculated. An interferogram is an electrical signal depicted as a function of the time delay (retardation) of the two beams in the interferometer. The addition procedure improves the signal-to-noise ratio, since the noise level is inversely related to the square root of the number of scans. The average interferogram is then prepared through further processing, such as zero filling, phase correction, and apodization. The application of these mathematical techniques is necessary for the compensation of instrumental artifacts.

Fourier transformation is a decoding procedure by which the signal is converted from the so-called time domain, where the signal is a function of retardation, to the frequency domain, where it is a function of frequency, according to the formula:

$$S(\nu) = 2 \int_0^{\infty} I(x) \cos(2\pi \bar{\nu} x) dx,$$

where x is the retardation; $I(x)$, the interferogram; $\bar{\nu}$ is any wavenumber, and $S(\nu)$, the spectrum.

4.1.1.4 Advantages of FTIR Spectroscopy

Signal-to-Noise Ratio and Linearity

FTIR spectroscopy has a high signal-to-noise ratio; this is the most important advantage of this type of spectroscopy, caused partly because all spectral elements (wavelengths) are observed simultaneously during the whole recording time. By contrast, in grating spectrometers only one resolution element can be examined at a time. The signal-to-noise ratio improves with the square root of the observation time of each resolution element, $\bar{\nu}$. The signal-to-noise advantage that the interferometer offers for a spectral region S between $\bar{\nu}_1$ and $\bar{\nu}_2$ is equal to $(S/\Delta\nu)^{1/2}$. This is called multiplex advantage. Another reason for the better signal-to-noise ratio is the high optical throughput in FTIR spectrometers, which is about 200 times higher than for dispersive IR spectroscopy. This is referred to as the throughput advantage. The combined multiplex and throughput advantages results in a high dynamic range of linearity, making FTIR spectroscopy most suitable for quantitative work.

Accuracy

The high accuracy in frequency, often referred to as laser reference advantage, is a result of using laser technology for coordinating the mirror movement and data recording. This is, however, more important for gas phase investigations than for studies of lignins and lignocellulosics. Nevertheless, high accuracy is also indispensable for data handling, such as in spectral subtraction.

Data Handling Facility

The advent of computer-controlled FTIR spectrometers has accelerated the use of software for spectral data manipulation, which is particularly beneficial in the study of lignin and lignocellulosics. Well-designed routine programs permit the following operations: (1) base line correction and normalization of spectra, a prerequisite for intra- and interlaboratory comparisons of spectra and for the use of automatic library search programs; (2) subtraction of interfering absorbances, which is important for analyzing the composite spectra of lignocellulosics; (3) expansion of co-ordinates, which is useful for magnifying spectral details of interest; (4) application of mathematical resolution techniques such as derivative spectroscopy (first and second derivatives), deconvolution, and band-fitting (band shape analysis); and (5) statistical analysis such as partial least squares (PLS), principal components analysis (PCA), and other methods often included with the manufacturer's software, that are very useful quantitative or semi-quantitative tools for analysis of multiple components.

Mechanical Simplicity

The mechanical simplicity of an FTIR spectrometer contrasts sharply with its theoretical complexity. The only moving part is the mirror, which rides on air or mechanical bearings to facilitate maintenance and improve reliability. The round cross-section of the FTIR beam is especially advantageous in situations where a circular attenuated total reflectance (CATR) accessory for liquids is used. For heat-sensitive compounds it is important to note that the sample is not heated significantly during the FTIR measurement.

There is a large body of literature on FTIR spectroscopy including, for example, Bracewell (1965), Horlick (1968), Bell (1972), Griffiths (1975, 1983), Ferraro and Basile (1978), Koenig (1981), Griffiths and de Haseth (1986), Perkins (1986, 1987), Mackenzie (1988). Cameron and Moffatt (1984), and Gillette et al. (1985) have explained the basic mathematical concepts of deconvolution, derivation and smoothing in FTIR spectroscopy.

4.1.2 Method

4.1.2.1 FTIR Spectroscopy in Practice

At present, the manufacturers listed below deliver reliable instruments with satisfactory working software. The type of instruments and models are not listed because the models change frequently and the software is updated almost annually. Users may select from a variety of beam splitters, detectors, computer memory, and software. The entire spectral range, from the far infrared through the near infrared, is covered by various FTIR instruments. Instrument suppliers include Analect (USA), Bomem (Canada), Bruker (FRG), Bio-Rad, Digilab Division (USA), Mattson (USA), Jasco (Japan), Nicolet (USA), and Perkin-Elmer (UK). Accessory manufacturers include Spectra-Tech Inc. (USA), Specac (UK, USA), Harrick Scientific Corp. (USA), and AAB SPEC (USA).

Figure 4.1.2 shows several elements of FTIR spectroscopic measurements with which one needs to become familiarized before proceeding, namely the interferogram, the appearance of the single beam spectrum composed of instrumental artifacts and the spectrum of air in the mid-IR range using a DTGS detector, and the so-called “100% line” between 2200 and 2000 cm^{-1} . The size and shape of interferogram is optimized by adjusting the instrument. The maximum intensity of the interferogram is called the centerburst. Ideally, it should be matched to the analog-digital-computer (ADC) and should have a peak form. The centerburst optimization should be repeated if accessories with high energy consumption (e.g., reflectance techniques, micro sampling) are used. The single-beam spectrum provides, besides background interference data specific to the instrument, constant information on the humidity and CO_2 content of the air. Using a standard DTGS detector, the response at 4000 cm^{-1} should be 20% of that at 1800 cm^{-1} . The magnified section of a transmission spectrum of an empty beam (100% line) recorded with 8 cm^{-1} resolution between 2200 and 2000 cm^{-1} provides information on the noise contributed by

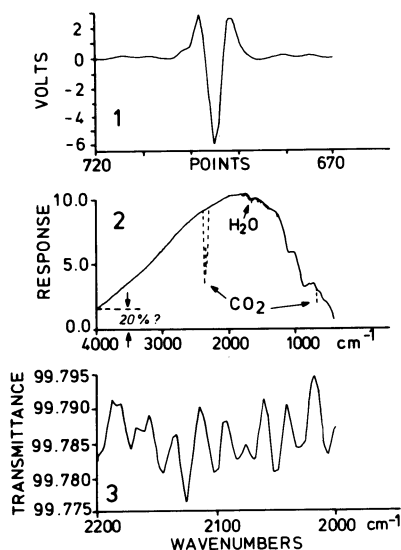


Fig. 4.1.2. Important elements of a FTIR spectroscopy. 1 Interferogram. 2 Single-beam spectrum. 3 100% line

the instrument. Because of the complexity of the adjustment procedure, which varies from instrument to instrument, consultation of the operating manual is always necessary.

4.1.2.2 Procedures

Lignin IR spectra are easy to obtain routinely. As a rule of thumb, one should use the KBr transmission technique (TR) for routine work wherever possible. Reflection techniques, e.g., attenuated total reflectance (ATR) or diffuse reflectance (DR), are methods for dealing with special problems, such as liquids or high consistency pastes, and surface investigations in the solid state. The same is true for photoacoustic (PA) methods. TR, DR, and microsampling techniques are addressed below because of their importance in lignin and wood chemistry. ATR and PA methods are less used for the characterization of pure lignins. Details of the PA technique have been discussed by Rosencwaig (1981), Graham et al. (1985), Harbour et al. (1985), Kuo et al. (1988) and Oelichmann and Hauser (1988).

Sample Preparation in the Transmission Mode

The most common way to obtain IR spectra for quantitative evaluation is to embed the sample in an alkali halide pellet. Dry, spectroscopy-grade potassium bromide or potassium chloride are suitable embedding media. (Drying procedure: 120°C in oven for at least 1 h, followed by cooling in a desiccator over

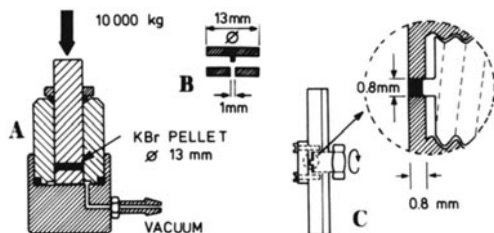


Fig. 4.1.3A–C. Preparation of alkali halide pellets. **A** Press for preparation of standard (macro) pellets. **B** Adapter for preparation of micro pellets. **C** Adapter and sample holder for micro pellet

P_2O_5). A standard 13-mm diameter pellet is prepared by pressing a 1–2 mg sample in 350 mg of KBr in an evacuated die (Fig. 4.1.3A).

The IR spectrum of a blank pellet is recorded and stored in the computer memory as background. The spectrum of the blank reveals whether the effort to remove water has been successful. Water has signals at about 1625 and 3700 cm^{-1} . The finer the powder, the greater the amount of water that can be adsorbed in a given time. A detailed water/KBr interaction has been provided by Malhotra et al. (1989). The KBr should not be ground in a mortar or milled for an unnecessarily long time to avoid water uptake. The use of a glove box with dry air purge is highly recommended in special cases. However, for routine runs, a small amount of water in the pellets can be tolerated if both sample and blank pellets are prepared in exactly the same way. In such cases, the water peak is cancelled out by subtracting the spectrum of the blank from that of the sample. A heated die also helps to avoid water in the pellet.

The band resolution in the carbonyl stretching region can be improved relative to that obtained in the KBr technique through use of the paraffin or fluorocarbon oil-mull method, also known as the Nujol technique (Hergert 1971). In this procedure, the sample is milled uniformly in an agate mortar together with a few drops of oil. The spectrum is then run as an oil suspension sandwiched between salt plates especially constructed for this purpose. This technique is recommended only for situations in which the carbonyl regions are of interest since the C—H bonds in the hydrocarbons of the mulling medium cause spectral interference.

Diffuse Reflectance (DR)

Infrared light is partly reflected from the surface and partly transmitted to a depth of a few micrometers in powdered material. The light that enters the material is absorbed or scattered. The re-emitted light has components from the surface and layers close to the surface. This phenomenon, in which the light is reflected in many different directions, is termed diffuse reflectance (DR). In an ideal case, the energy distribution of the diffusely reflected light is homogeneous irrespective of the reflection angle. Another mode of reflection is the regular,

mirror-like reflection normally observed with smooth surfaces and described as specular reflection. When measuring diffuse reflectance, the specular component of reflection should be reduced as much as possible since these two reflection modes obey different laws.

Low levels of reflected energy, even from micro samples, can be measured by FTIR instruments. This method is termed diffuse reflectance infrared Fourier transform (DRIFT) spectroscopy. A reflectometer design with hemiellipsoidal mirrors sliding back for sample positioning is very convenient (Fig. 4.1.4).

For DRIFT studies, a wood wafer, paper sheet, or milled wood sample dispersed in KBr (or KCl) is placed in a cup at the focal point of the concave, ellipsoidal mirror so that the incident light is focused on the sample. The scattered light coming from the sample is collected from the concave mirror and directed by a suitable mirror system to the detector of the FTIR instrument. The pressure used for smoothing the sample has to be adjusted so that reproducible results can be obtained (Yeboah et al. 1984). The contribution of specular reflectance can be diminished by reducing the particle size and by increasing the sample dilution. For powder samples, as indicated above, the diluent is KBr or KCl. Good results are normally obtained with alkali halide powders that contain 1–2% of sample. In certain cases, the sample concentration may be increased up to 10%.

When measuring paper sheets or wood surfaces, the so-called Blocker device (Spectra-Tech Inc.) must be used to eliminate the specular light. Surface quality often influences the results. For example, DRIFT spectra are slightly different when taken on the top side or the wire side of a paper sheet.

DRIFT spectroscopy is of special interest in studying wood surface phenomena, for example, the effects of oxidation, photooxidation, and weathering. Moreover, it is advantageous for the analysis of highly absorbing materials

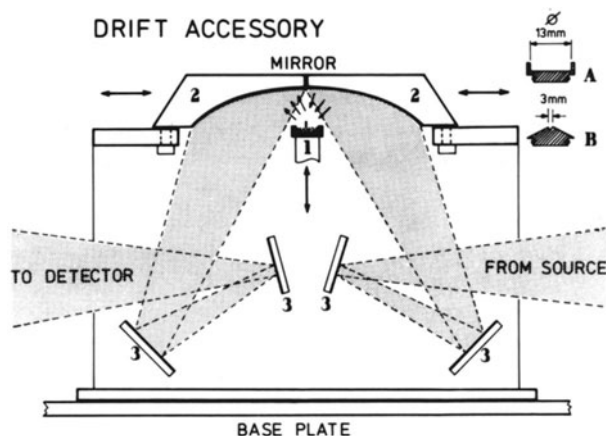


Fig. 4.1.4. Diffuse reflectance accessory (Spectra-Tech Inc.). 1 Movable stage with Blocker device to diminish the specular component of reflectance; 2 two movable parts of the hemiellipsoidal mirror. The mirror opens for sample positioning; 3 mirror system to reflect the IR beam from the source to the detector; A macro sample holder; B micro sample holder

such as charcoal or technical lignins. DRIFT is also well suited for infrared microsampling in GPC and HPLC analyses.

A general description of DRIFT has been provided by Ferraro and Rein (1985). The application of DRIFT to wood, pulp, and lignin chemistry has been discussed by Schultz et al. (1985a,b), Schultz and Glasser (1986), Yang et al. (1986), Berben et al. (1987), Grandmaison et al. (1987), Faix and Németh (1988), Hauser and Oelichmann (1988), Michell (1988a,b), Michell et al. (1989) and Ostmeyer et al. (1989).

Micro Techniques

The need for micro sampling often arises from the morphological and chemical inhomogeneity of wood. The sample size for DRIFT can be reduced to nanograms by using a micro cup (see Fig. 4.1.4). Manufacturers of accessories also offer devices for the preparation of KBr discs ranging down to 1 mm diameter (see Fig. 4.1.3 B and C). Micro pellets are usually prepared in a small agate mortar as described above for the preparation of macro pellets. Diamond anvil cells are useful for micro analysis of wood fibers. In these cells, sample thickness may be reduced by the application of pressure. Optimal adjustment of the instrument is especially important in micro analysis. Sample positioning has to be optimized in the "set up" mode of the instrument. This is done by observing the interferogram while adjusting the sample holder. As is true for all accessories, the highest interferogram response indicates optimal positioning. Incorrectly oriented samples may result in irregularities such as vignetting and interference fringes.

For very small samples (in the picogram range, or with disc diameters below 0.5 mm), the use of a FTIR microscope is required. A FTIR microscope is schematically shown in Fig. 4.1.5 for Bio-Rad Digilab Model UMA 300 A. The microscope permits visual inspection of the sample for selecting a spot of

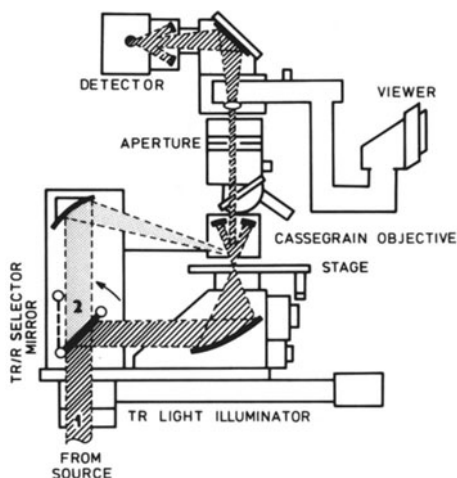


Fig. 4.1.5. FTIR microscope UMA 300 A (Bio-Rad, Digilab) operating in the transmission 1 or in the reflectance 2 mode

interest. The spectrum is recorded only from this part of the object by focusing the infrared beam on the sample with the switchable objective. After being transmitted through the sample, the IR beam is collected by a Cassegrain mirror objective. The Cassegrain objective works on the principle of reflection since the standard microscopic transmission objective of glass or quartz, used for the visible-range measurements, cannot be used in IR spectroscopy. A photo-conductivity detector made of mercury cadmium-telluride (MCT) with a small collecting area collects the transmitted IR beam.

The resolution, R , depends on the numerical aperture, NA , and the wavelength, λ , according to the formula

$$R = \frac{\lambda(\text{in } \mu\text{m})}{NA}.$$

R is approximately between 4 and $30\mu\text{m}$ in the mid-IR range ($2.5\text{--}20\mu\text{m}$) when $NA = 0.70$. Sometimes it is possible to obtain IR spectra of good quality for samples with dimensions below the theoretical limits. The high diffraction effects of Cassegrain objectives may require the use of two apertures, one below and the other above the sample, to minimize the diffraction in the transmission mode.

Spectra of good quality normally can be obtained in a reasonably short measuring time (less than 5 min) with disc diameters ranging from $20\text{--}30\mu\text{m}$. FTIR microspectroscopy is described by Fuller and Griffiths (1980), Bartick (1985), Krishnan (1988), Schiering et al. (1988), Sommer et al. (1988) and Sweeney (1989).

4.1.3 Lignin Characterization in the Mid-Infrared Region ($4000\text{--}500\text{ cm}^{-1}$)

4.1.3.1 Band Assignment and Classification of Lignin IR Spectra

Table 4.1.1 lists band assignments for the FTIR spectra of three different milled wood lignins, namely guaiacyl-type (G), guaiacyl/syringyl-type (GS), and hydroxyphenyl/guaiacyl/syringyl-type (HGS). Only a few group frequencies and bands are unequivocally assigned, and many bands can be interpreted in various ways. The O—H, C—H, and C=O stretching modes above 1600 cm^{-1} and the aromatic skeletal vibration around 1510 cm^{-1} are “pure” bands, whereas the 1600 cm^{-1} aromatic skeletal vibration band is a superimposed band that has been broadened by the C=O stretching mode (Hergert 1971). Interpretation of the bands below 1430 cm^{-1} is more difficult. Here, nearly all bands are complex, with contributions from various vibration modes.

The band wavenumbers in Table 4.1.1 were obtained at 4 cm^{-1} resolution. The intensity values shown in the parentheses were obtained from baseline-corrected and standardized spectra (Figs. 4.1.6 and 4.1.7). As shown in Fig. 4.1.7, most IR bands are common to the three main lignin types although their intensities may differ. In the wavenumber range $2700\text{--}3700\text{ cm}^{-1}$, the band intensities of all lignin types are similar (Table 4.1.1, Fig. 4.1.6).

A semi-quantitative comparison of band intensities can be used for lignin classification as first described by Kawamura and Higuchi (1964a,b).

Table 4.1.1. Band assignments in the mid-infrared region of nonderivatized G, GS, and HGS-type milled wood lignins. Band intensities (*in parenthesis*) were measured from the zero line of baseline-corrected and normalized spectra. Intensity of the highest band equals 100

Wavenumbers (cm ⁻¹) Baseline (Abs. = 0)	No. in Fig. 4.1.7	Band origin, short comments	Maxima at cm ⁻¹ , % absorbance (% A) from standard spectra					
			Spruce MWL		Beech MWL		Bamboo MWL	
	Range of maxima		cm ⁻¹	% A	cm ⁻¹	% A	cm ⁻¹	% A
from 3695 to 3042	3412–3460	1 O—H stretch	3412	(58)	3460	(49)	3428	(45)
	3000–2842	2 C—H stretch in methyl and methylene groups	3000 2937 2879 2840	(5) (24) (15) (12)	3000 2940 2880 2840	(7) (22) (12) (12)	3002 2942 2879 2840	(6) (22) (11) (11)
to 2782 from 1800	1738–1709	3 C=O stretch in unconjugated ketones, carbonyls and in ester groups (frequently of carbohydrate origin); conjugated aldehydes and carboxylic acids absorb around and below 1700 cm ⁻¹	1722	(11)	1735	(18)	1709	(45)
	1655–1675	4 C=O stretch; in conjugated p-subst. aryl ketones; strong electronegative substituents lower the wavenumber	1663	(29)	1658	(23)		
	1593–1605	5 aromatic skeletal vibrations plus C=O stretch; S > G; G condensed > G etherified	1596	(46)	1593	(54)	1601	(75)
	1505–1515	6 aromatic skeletal vibrations; G > S	1510	(95)	1505	(60)	1511	(77)
	1460–1470	7 C—H deformations; asym. in —CH ₃ and —CH ₂ —	1464	(60)	1462	(63)	1462	(68)
	1422–1430	8 aromatic skeletal vibrations combined with C—H in-plane deform.	1423	(53)	1422	(53)	1423	(56)

1365–1370	9	aliphatic C—H stretch in CH ₃ , not in OMe; phen. OH	1367	(33)	1367	(27)		
1325–1330	10	S ring plus G ring condensed; (i.e., G ring substituted in pos. 5)	1326	(38)	1329	(48)	1329	(57)
1266–1270	11	G ring plus C=O stretch	1269	(100)	1266	(48)	1267	(80)
1221–1230	12	C—C plus C—O plus C=O stretch; G condensed > G etherified	1221	(70)	1227	(67)	1229	(81)
1166	13	typical for HGS lignins; C=O in ester groups (conj.)		(78)			1166	(71)
1140	14	aromatic C—H in-plane deformation; typical for G units; whereby G condensed > G etherified	1140					
1128–1125	15	aromatic C—H in-plane deformation (typical for S units); plus secondary alcohols plus C=O stretch			1126	(100)	1127	(100)
1086	16	C—O deformation in <i>secondary alcohols</i> and aliphatic ethers	1086	(45)				
1030–1035	17	aromatic C—H in-plane deformation, G > S; plus C—O deform. in primary alcohols; plus C=O stretch (unconj.)	1032	(76)	1033	(54)	1032	(58)
966–990	18	—HC=CH— out-of-plane deform., (trans)						
915–925	19	C—H out-of-plane; aromatic	919	(5)	925	(20)		
853–858	20	C—H out-of-plane in position 2, 5, and 6 of G units	858	(11)				
834–835	21	C—H out-of-plane in position 2 and 6 of S, and in all positions of H units			835	(10)	834	(26)
817–832	22	C—H out-of-plane in positions 2, 5, and 6 of G units			817	(8)		
to 780								



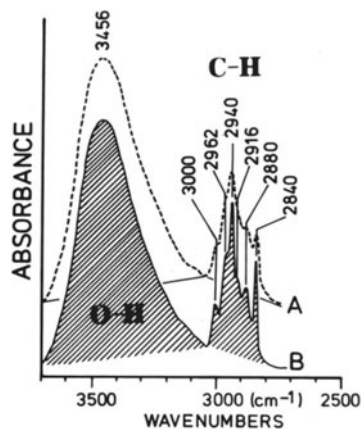


Fig. 4.1.6. O—H and C—H stretching bands of European beech (*Fagus sylvatica*) MWL. *A* 4 cm^{-1} resolution; *B* spectrum after mathematical resolution enhancement using deconvolution technique. (Experimental conditions described in legend to Fig. 4.1.11)

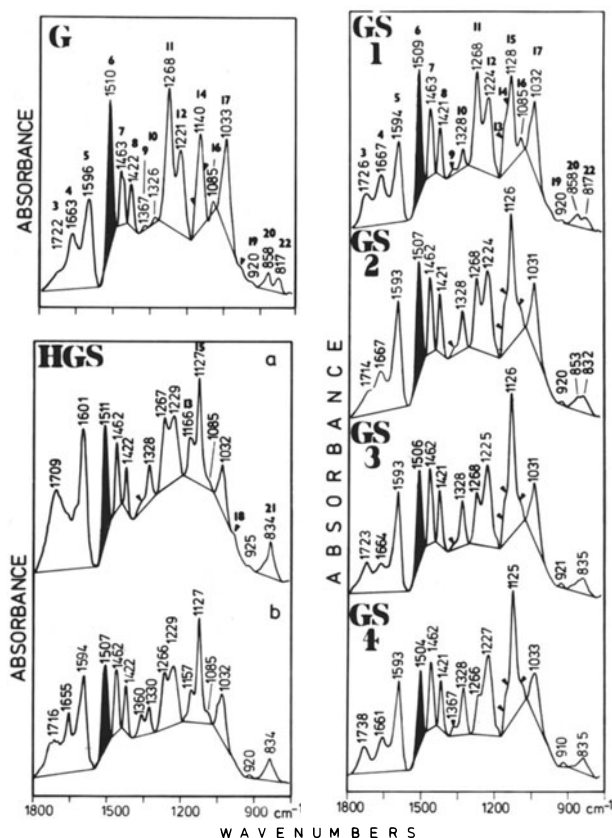


Fig. 4.1.7. Baseline-corrected and normalized FTIR spectra illustrating spectral types G, GS 1-GS 4, and HGS. *G* Norway spruce (*Picea abies*); *GS 1* (*Gnetum venosum*); *GS 2* lauan (*Shorea polysperma*); *GS 3* dabema (*Piptadeniastrum africanum*); *GS 4* birch (*Betula* sp.); HGS *a* bamboo (*Bambusa* sp.); *b* barley (*Hordeum vulgare*). (Instrument: FTS 40 Bio-Rad, Digilab, 4 cm^{-1} resolution, 32 scans, KBr pellet technique). According to Faix 1991

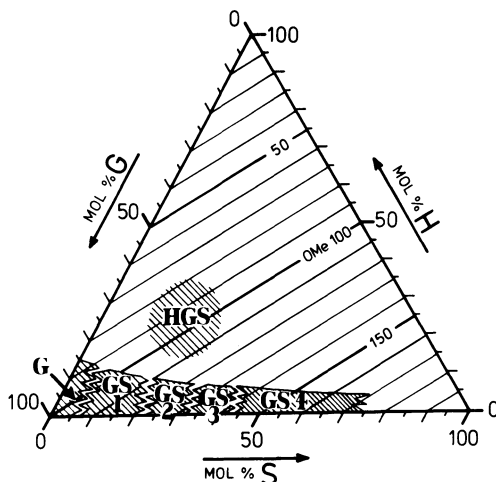


Fig. 4.1.8. Triangular coordinate system displaying the three types of lignin (G, GS, and HGS) in relation to the composition of the lignins (H, G, and S units expressed as mol % and the methoxyl contents as the number/100 phenylpropane units). According to Faix 1991

In Fig. 4.1.7, the GS-type is subdivided into four subgroups based on the ratio of the 1509/1462 and 1268/1224 bands. The spectral differences are mostly the result of variation in the H, G, and S ratios in lignin. For simplicity, the three lignin types and the four subgroups, GS1–GS4, are described by a triangular coordinate system (Fig. 4.1.8) based on the contents of the basic lignin building units (i.e., G, S, and H units). In agreement with earlier studies (Sarkanen and Ludwig 1971), most wood lignins belong to the GS type containing trace amounts of H units. The S content of GS-type lignins may vary from a few percent to 70%. The HGS type is isolated from the other two types and has an H content of 15 to 20% and an S content of about 20%. This subject has been discussed in greater detail by Faix (1991).

4.1.3.2 Influence of Carbonyl Groups

As shown in the above section, the ratio of H, G, and S units exerts a major influence on the characteristics of lignin IR spectra. Carbonyl groups (bands 3 and 4) also show dominant effects, particularly in bands 5, 11, 12, 13, and 17. The effects usually are eliminated by reduction, as indicated by the so-called NaBH_4 -reduction difference spectrum shown in Fig. 4.1.9. Sodium borohydride reduction decreases the band intensity at $1724\text{--}1741\text{ cm}^{-1}$ (all samples), 1668 cm^{-1} (*Picea abies*), 1602 cm^{-1} (bamboo), 1593 cm^{-1} (*Picea abies*), $1270\text{--}1230\text{ cm}^{-1}$ (all samples), and $1170\text{--}1127\text{ cm}^{-1}$ (all samples), resulting in positive peaks in the difference spectra. The bands at 3500 , 3200 , 2930 , $1610\text{--}1620$, 1516 , 1202 , $1100\text{--}1110$, and 1014 cm^{-1} increase in intensity, resulting in the negative peaks. Figure 4.1.10 is a compilation of $\text{C}=\text{O}$ group assignments for lignin model compounds. Unsaturated aliphatic esters are not reduced by

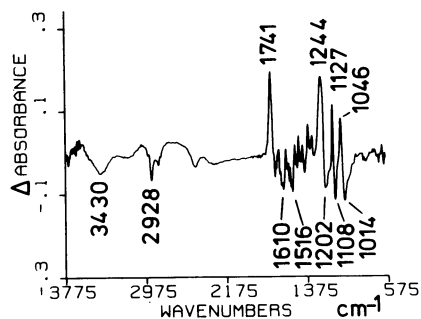


Fig. 4.1.9. Difference spectrum of oak (*Quercus obtusata*) obtained by subtracting the spectrum of MWL from the spectrum of the same MWL after NaBH_4 reduction. (Instrument: Nicolet 20SX D, 4 cm^{-1} resolution, 32 scans, KBr pellet technique)

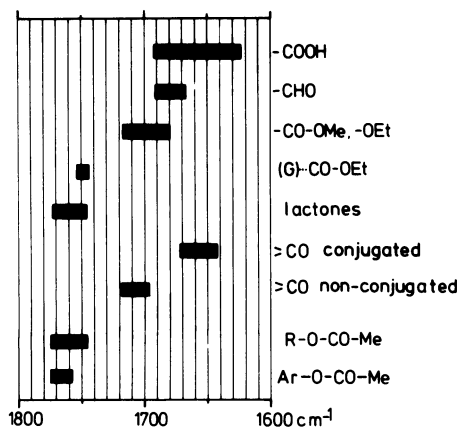


Fig. 4.1.10. Range of carbonyl group vibrations observed in lignin model compounds

NaBH_4 and the carboxyl bands are shifted to $1590\text{--}1560\text{ cm}^{-1}$ upon conversion to their sodium salts. Water present in KBr pellets gives rise to a signal at 1625 cm^{-1} , which may interfere with the conjugated $\text{C}=\text{O}$ band. A high signal intensity in the $1700\text{--}1760\text{ cm}^{-1}$ range often indicates the presence of hemicellulose in milled wood lignin. Phenolic acid esters, especially in grass lignins, may also contribute to the signal in this range.

4.1.3.3 Mathematical Resolution of Spectra

In the spectra of macromolecules, the overlapping bands cannot be resolved by instrumental manipulation alone. Instead, mathematical techniques such as deconvolution, derivative spectroscopy, and band fitting are used for improving the spectral quality.

Deconvolution

Deconvolution is manipulation of the interferogram with an exponential weighting function. It may be viewed as the inverse of smoothing. In deconvoluted

spectra, shoulders and points of inflection become peaks, and narrow bands are sharpened. For theoretical reasons, few advantages can be expected from the very broad composite carbonyl bands of lignin at $1630\text{--}1750\text{ cm}^{-1}$, and no effect can be seen on the OH band (Fig. 4.1.6). Moreover, the spectra frequently show background noise in the carbonyl region due to traces of vapor in the instrument and adsorbed water in the pellet. This is a serious limitation because a high signal-to-noise ratio is a prerequisite for successful deconvolution.

Deconvolution provides a better indication of the approximate number of individual components contributing to a superimposed band. Figure 4.1.11 shows the spectra of three milled wood lignins before and after deconvolution (Faix and Beinhoff 1988). Table 4.1.2 lists the wavenumbers and intensities of bands after deconvolution. The band intensities change when a different band width is used for the deconvolution, but the band positions (wavenumbers) remain constant.

Derivative Spectroscopy

First derivative IR spectra of a softwood and hardwood lignin are shown in Fig. 4.1.12. They display 20–22 positive and negative peaks instead of the 12 to 14 maxima appearing in the original spectra. Broad bands with low intensity are

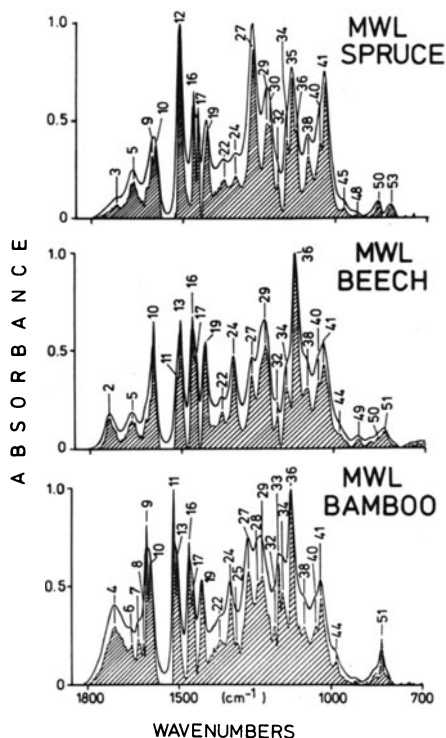


Fig. 4.1.11. FTIR spectra of spruce, beech, and bamboo MWL before and after deconvolution (Faix and Beinhoff 1988). (Instrument): Bio-Rad, Digilab FTS 40, resolution 4 cm^{-1} , 64 scans, bandwidth for deconvolution 15 cm^{-1} , KBr pellet technique). By courtesy of Marcel Dekker Inc.

Table 4.1.2. Wavenumbers and intensities of IR bands after enhanced resolution obtained by deconvolution; bandwidth for deconvolution, 15 cm⁻¹. According to Faix and Beinhoff 1988, by courtesy of Marcel Dekker Inc.

Band #		x cm ⁻¹	MWLs						Remarks
4.1.7	4.1.11		Spruce cm ⁻¹	% A	Beech cm ⁻¹	% A	Bamboo cm ⁻¹	% A	
3	1	1771							in GS DHPs
	2	1737	1737	(4)	1737	(17*)	1737	(18)	
	3	1720	1718	(7*)	1718	(10)	1718	(25)	
	4	1710	1710	(5)	1710	(5)	1710	(30*)	
4	5	1664	1664	(19*)	1664	(16*)	1664	(19)	
	6	1654					1655	(21*)	
	7	1634					1634	(24*)	
5	8	1614	1616	(16)	1617	(16)	1616	(21*)	
	9	1604	1604	(33*)	1604	(26)	1605	(82*)	
	10	1593	1593	(37*)	1592	(67*)	1593	(62*)	
6	11	1516			1515	(38*)	1515	(100*)	in G DHPs
	12	1511	1511	(100*)					
	13	1505			1504	(67*)	1504	(65*)	
	14	1498							
	15	1493	1493	(12)					
7	16	1465	1465	(66*)	1465	(69*)	1465	(73*)	
	17	1453	1451	(58*)	1455	(48*)	1453	(49*)	
8	18	1428	1427	(28)			1428	(15)	
	19	1422	1421	(46*)	1421	(56*)	1422	(52*)	
9	20	1384	1384	(16)			1384	(19*)	in DHPs
	21	1373							
	22	1367	1366	(20*)	1368	(18*)	1365	(23*)	
	23	1344							
10	24	1329	1328	(22*)	1328	(46*)	1329	(44*)	in DHPs
	25	1311					1311	(21*)	
	26	1290					1290	(29)	
11	27	1270	1269	(87*)	1270	(38*)	1269	(58*)	
12	28	1239			1240	(47)	1237	(52*)	
	29	1225	1224	(49*)	1224	(54*)	1225	(56*)	
	30	1214	1215	(48*)					
	31	1204					1204	(37*)	
	32	1186	1189	(18*)	1185	(17*)	1184	(31*)	
13	33	1170					1170	(63*)	
	34	1157	1158	(41*)	1154	(32*)	1158	(48*)	
14	35	1143	1141	(72*)					
15	36	1128	1128	(46*)	1128	(100*)	1127	(100*)	
	37	1104					1104	(31*)	
16	38	1086	1089	(33*)	1086	(32*)	1088	(30*)	in DHPs
	39	1057							
17	40	1048	1048	(39*)	1048	(34*)	1048	(31*)	
	41	1032	1031	(70*)	1032	(44*)	1031	(45*)	
	42	1020	1020	(24)	1020	(34)	1020	(24)	

Table 4.1.2. (continued)

Band #		MWLs						Remarks
4.1.7	4.1.11	x cm ⁻¹	Spruce cm ⁻¹	% A	Beech cm ⁻¹	% A	Bamboo cm ⁻¹	
18	43	991						in GS DHPs
	44	982			981	(8*)	984	
	45	972	972	(6*)				
	46	966						in G DHPs
	47	945						
19	48	926	927	(2*)				in G DHPs
	49	920			918	(6*)	922	
20	50	854	856	(10*)	854	(7*)	854	(7*)
21	51	831			834	(9*)	834	(24*)
22	52	822						in G DHPs
	53	816	816	(7*)			815	
	54	704						in GS DHPs

Bands labeled with * show a maximum. A = Absorbance of normalized spectra. "A" for the highest band equals 100. (Instrument: Bio-Rad, Digilab FTS 40)

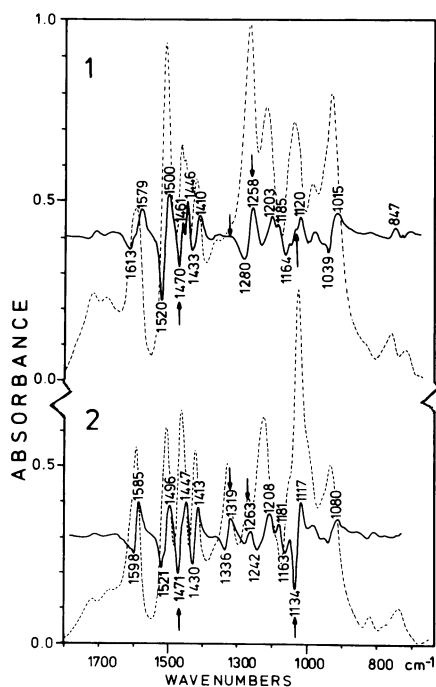


Fig. 4.1.12. IR spectra (dotted line) and first derivative IR spectra of two Willstätter lignins. 1 Bald cypress (*Taxodium distichum*), example of a G lignin; 2 tulip tree (*Liriodendron tulipifera*), example of a pronounced hardwood (GS 4) lignin

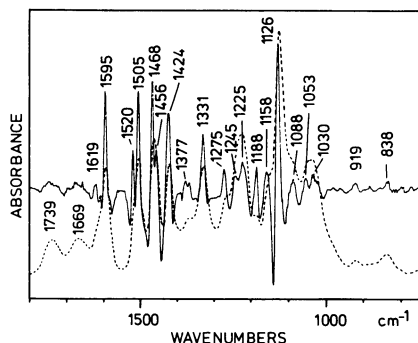


Fig. 4.1.13. IR spectrum (dotted line) and second derivative IR spectrum of tulip tree (*Liriodendron tulipifera* sapwood MWL. (Resolution 4 cm^{-1} , 64 scans, KBr pellet technique)

suppressed and the disturbing effect of a tilted baseline disappears. A disadvantage is that the resulting spectra display no similarity with the original. Despite this, first derivative spectra can be evaluated quantitatively. The peaks labeled with an arrow, for example, clearly highlight the differences between G and GS lignins. However, information on the carbonyl groups is lost in the derivatization. Figure 4.1.13 displays the original and the second derivative spectra of a hardwood MWL. At least 26 positive major peaks are visible in full conformity with the results of the deconvolution data presented in Table 4.1.2. Deconvolution and second derivative spectra give exactly the same wave numbers for the bands arising from the increase resolution. The use of second derivative IR spectroscopy for characterization of celluloses and technical lignins has been reported by Michell (1988d).

Band Fitting

Band fitting (curve fitting, or band shape analysis) is conveniently performed with commercially available software packages which fit, interactively or automatically, Gaussian or Lorentzian line shapes (or their combinations) to an unknown band profile. The applicability of this technique to lignin chemistry is not known at present.

4.1.3.4 Effect of Acetylation

Derivatization of lignin often discloses hidden features of IR spectra. A difference spectrum of acetylated lauan (*Shorea polysperma*) MWL, shown in Fig. 4.1.14, demonstrates the effects of acetylation. The OH band at $3410\text{--}3460\text{ cm}^{-1}$ disappears upon acetylation; acetoxy bands appear at $1765\text{--}1772\text{ cm}^{-1}$ (shoulder, aromatic), 1743 cm^{-1} (aliphatic), 1371 cm^{-1} , as do peaks in a cluster with maxima at 1217 , $1225\text{--}1227$, and 1198 cm^{-1} . It is noteworthy

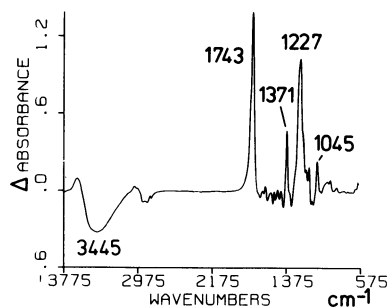


Fig. 4.1.14. Difference spectrum obtained by subtracting the spectrum of acetylated red lauan (*Shorea polysperma*) MWL from the spectrum of the same MWL before acetylation. (Resolution 4 cm^{-1} , 64 scans, KBr pellet technique)

that a sub-band of the aromatic band at 1518 cm^{-1} also disappears upon acetylation. (This effect can be seen only in the spectrum of the acetylated lignin).

In the spectra of acetylated organosolv lignins (i.e., lignin solubilized through partial splitting of its interunit ether linkages by alcohols), additional maxima appear at 1600 , 1131 , and 1044 cm^{-1} . The ratio of the acetoxy bands $1765/1743\text{ cm}^{-1}$ can be used for estimating the ratio of phenolic/aliphatic OH groups, as illustrated in Fig. 4.1.15. In this case, the pure acetoxy groups from acetylated lignins are shown before and after deconvolution. The increase in the phenolic hydroxyl group content of the organosolv lignin resulting from β -0-4 splitting reactions is clearly shown. The usefulness of FTIR spectroscopy for the structural analysis of acetylated lignins has been documented by Schultz and Glasser (1986).

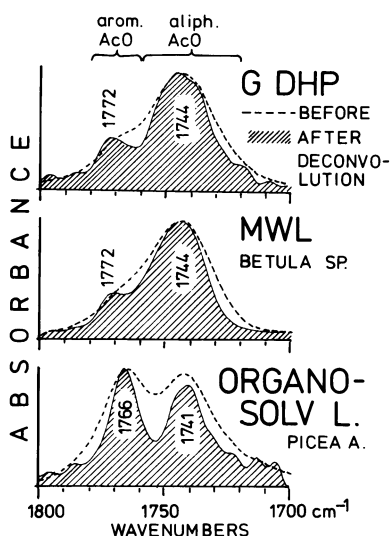


Fig. 4.1.15. Acetyl bands of acetylated lignins before and after deconvolution (Faix 1987). Acetylation in Ac_2O /pyridine. (Conditions described in legend to Fig. 4.1.11 caption)

4.1.3.5 Quantitative Evaluation

FTIR spectroscopy furnishes rather comprehensive data for quantitative work, even though the overlapping of bands occasionally is a limiting factor. The procedure for quantitative evaluation consists of several phases as described below.

Generation of IR Data Sets

IR spectra of lignin can be presented in three forms, namely as raw spectra, as baseline-corrected raw spectra, and as baseline-corrected normalized spectra. The band heights are determined from either the absolute zero line or from a baseline. In the latter case, there are again two possibilities: measurement of the heights of two or more bands from one common baseline or from the construction of an individual baseline for each band constructed by connecting the left side minimum with the right side minimum of the particular band. If an "individual" baseline is constructed, the integrated area below this band can be used for quantification. Better interlaboratory comparability is achieved with data taken from baseline-corrected and normalized spectra, provided that the baseline correction is always made in the same way. Even with the normalized spectra, it is advantageous to select an internal standard band for calculating the relative band intensities of all absorption bands. The aromatic skeletal vibration band at $1505\text{--}1510\text{ cm}^{-1}$ is conventionally used as a reference band, but the bands at 2900 , 1463 , or 1420 cm^{-1} also may be used. Schultz et al. (1985a, and Schultz and Glasser 1986), for example, selected band numbers 5, 6 and 8 in Table 4.1.1 as the internal standards for generating IR data sets whereas Zavarin et al. (1982) used the 1420 cm^{-1} band for internal standardization. Nevertheless, the $1505\text{--}1510\text{ cm}^{-1}$ band should be used, if possible, to increase comparability.

The choice of the reference band (or bands), however, influences less the results than the reproducibility of the baseline construction and the correct reading of the maxima. Modern software in FTIR spectroscopy are useful in automatic and reproducible location of baselines, maxima, integral values, and baseline-corrected absorbances.

Reproducibility problems may arise when tangential baselines (for example on the right side of the 1033 cm^{-1} band) have to be constructed. As a rule, data sets generated on the basis of height measurements are as reliable and reproducible as those based on integral values. The reproducibility of relative band intensities in the transmission mode is, for most of the bands, about ± 0.5 to 1% . An exception is the 1600 cm^{-1} band which, because it is strongly influenced by humidity, exhibits poor reproducibility ($\pm 10\%$).

Sample preparation influences DRIFT spectra, as already pointed out. For example, dilution with KBr affects mainly the carbonyl region and the wave-number range between 1157 and 1046 cm^{-1} . Prolonged milling of the wood in KBr causes changes in the $1450\text{--}1046\text{ cm}^{-1}$ region (Fig. 4.1.16) as a result of decreased particle size. The use of KCl and NaCl as diluting media helps avoid noise in the carbonyl region resulting from moisture.

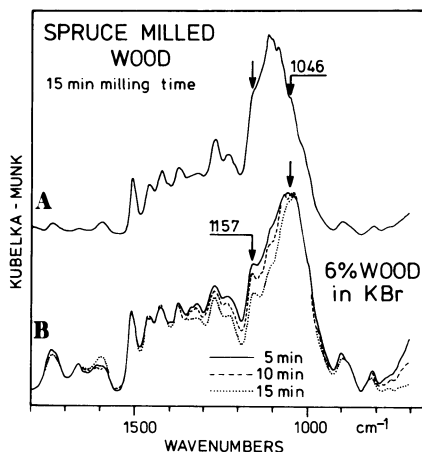


Fig. 4.1.16. DRIFT spectra of spruce milled wood. *A* Without dilution with KBr; *B* diluted with KBr (6% conc.) after 5, 10, and 15 min milling time in a vibratory ball mill

Calibration

The most important multivariate calibration techniques include multiple linear regression (MLR), principal component regression (PCR), and the partial least squares (PLS) method. All of these statistical techniques are used to arrive at a model that relates the IR data set (*R*) to the analytical data set (*C*). They are, in the given order, increasingly reliable with regard to mathematical stability and less sensitive to statistically irrelevant information. Under ideal conditions (i.e., when all bands show linear responses and there are no interfering signals and collinearities between the data), the above techniques give similar results. In practice, however, the PLS and PCR techniques have essential advantages (Beebe and Kowalski 1987).

The curve-fitting calibration technique is a process whereby sample spectra are modeled as linear combinations of constituent spectra. This procedure is better suited for the analysis of a mixture of known components than for complex biopolymers such as lignin. Nevertheless, ongoing successful work throughout the world on the calibration of FTIR data with those of wet chemistry demonstrates that FTIR spectroscopy can be a powerful tool for quantitative (or at least semi-quantitative) lignin analysis.

For additional information on multivariate calibration techniques, the reader should consult Antoon et al. (1979), Gillette (1983), Gillette et al. (1985), Sjöström et al. (1983), Frank et al. (1984), Naes and Martens (1984), Beebe and Kowalski (1987), Hirschfeld (1987), Compton et al. (1987), and Schultz et al. (1989).

For lack of space, the quantitative IR spectral evaluation of lignin cannot be dealt with in detail here. However, the literature surveyed below may help the reader to access this exciting new area of lignin chemistry. Sarkanen et al. (1967a,b) were the first to report on the quantification of IR spectroscopic data.

They observed a linear relationship when the relative IR band intensities of several NaBH_4 -reduced hardwood and softwood MWLs were plotted against their OMe contents. Later, several authors such as Faix and Schweers (1974), Kawamura et al. (1974, 1977), Lai and Sarkanen (1975), Salud and Faix (1980), Yasuda and Sakakibara (1981), Obst (1982), and Chum et al. (1984) reported on quantitatively evaluated IR spectra. Recently, the advent of FTIR spectroscopy has led to an increasing number of publications dealing with quantitatively evaluated IR spectra and their correlation with wet chemistry data, for example Schultz et al. (1985a,b), Faix (1986, 1987), Schultz and Glasser (1986), Schultz and Nicholas (1987), Abbott et al. (1988), Obst et al. (1989), and Owen and Thomas (1989). Schultz and Glasser (1986) and Grandmaison et al. (1987) have provided examples of quantitative data evaluation in DRIFT spectroscopy.

4.1.4 Lignin Spectra in the Near-Infrared Region ($4000\text{--}10\,000\text{ cm}^{-1}$)

FTIR spectra in the near-IR region consist entirely of overtones and combinations of primary bands within the mid-IR region. For macromolecules or complex mixtures, the excessive overlapping of bands produces a diffuse absorption continuum with few characteristic features, making unequivocal band assignment practically impossible. Thus, this spectral range has a limited use in qualitative analysis. Even so, a major asset of near-IR analysis is the ease with which reproducible spectra can be obtained by reflectance and transreflectance (a combination of transmission and reflectance) techniques in every state of aggregation without complicated sample preparation.

Figure 4.1.17a and b show near-IR spectra of milled softwoods and hardwoods and milled wood lignins isolated from the same wood. The envelopes of nonresolved overlapping bands originate mainly from the 1st, 2nd, and 3rd overtones of various types of C—H and O—H vibrations. There are only minor, but significant, differences between the spectra that are useful for quantitative analysis. Here, derivative spectroscopy is particularly beneficial for eliminating the tilted baselines and accentuating these small differences. Acetylation of milled wood lignin causes significant changes in the spectra (Fig. 4.1.17c).

Osborne and Fern (1986) have presented detailed band assignments in the near-IR range, and Wetzel (1983) and William and Norris (1987) have summarized the salient points of near-IR spectroscopy. The latter authors emphasize applications for the agricultural and food industries. Birkett et al. (1989) have reported the successful kappa number determination of pulps using spectra in the near-IR range.

4.1.5 Lignin Spectra in the Far-Infrared Region ($50\text{--}500\text{ cm}^{-1}$)

Very little information is available on lignin spectroscopy in this range. The spectra of beech and bamboo MWLs (Fig. 4.1.18) again show only diffuse bands originating from aromatic ring deformation vibrations. Sulfur-containing technical lignins display more pronounced features because of C—S vibrations.

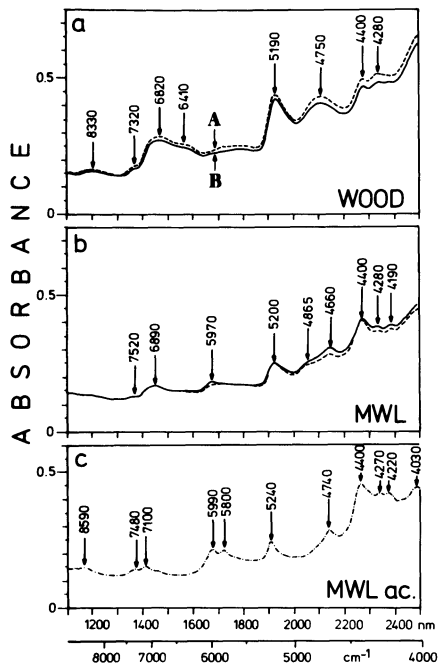


Fig. 4.1.17a–c. Near-infrared spectra. (a) Milled wood and MWL from common wingnut (*Pterocarya fraxinifolia*), hardwood lignin. (b) Milled wood and MWL from dawn redwood, (*Metasequoia glyptostroboides*). (c) Acetylated Norway spruce (*Picea abies*) MWL. (Instrument: Technikon Infralyzer 500; courtesy of E. Ignatzek, Bran & Luebbe, Hamburg)

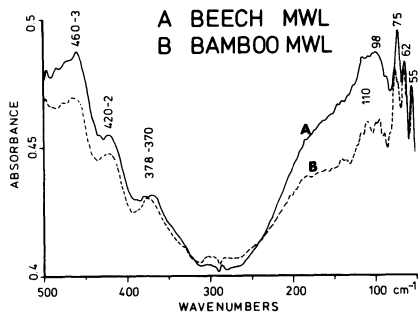


Fig. 4.1.18. Infrared spectrum of European beech (*Fagus sylvatica* L.) and bamboo (*Bambusa* sp.) MWLs in the near infrared range. (Instrument: Nicolet 7000; Resolution: 8 cm⁻¹, 128 scans; courtesy of J. Mink, Budapest)

4.1.6 Concluding Remarks

FTIR spectroscopy is a versatile, rapid, and reliable technique for lignin characterization. Baseline-corrected and normalized spectra facilitate interlaboratory comparisons. Using this analytical technique, the p-hydroxyphenyl, guaiacyl and syringyl units, methoxyl groups, carbonyl groups, and the ratio of phenolic OH to aliphatic OH groups can be determined. The DRIFT technique is well suited for wood surface characterization and lignin determination in wood and lignocellulosics in general, although its reproducibility is poor. Mathematical resolution techniques are useful for revealing hidden spectral information. However, FTIR spectroscopy in the near- and far-IR ranges needs further development.

References

- Abott TP, Palmer DM, Gordon SH, Bagby MO (1988) Solid state analysis of plant polymers by FTIR. *J Wood Chem Technol* 8:351–357
- Antoon MK, D'Esposito L, Koenig JL (1979) Factor analysis applied to Fourier transform infrared spectra. *Appl Spectrosc* 33:351–357
- Bartick EG (1985) Microscopy/infrared spectroscopy for routine sample size. *Appl Spectrosc* 39:885–890
- Beebe KR, Kowalski BR (1987) An introduction to multivariate calibration and analysis. *Anal Chem* 59:1007A–1017A
- Bell RJ (1972) Introductory Fourier transform spectroscopy. Academic Press, New York, 382 pp
- Berben SA, Rademacher JP, Sell LO, Easty DB (1987) Estimation of lignin in wood pulp by diffuse reflectance Fourier-transform infrared spectrometry. *Tappi J* 70(11):129–133
- Birkett M, Gambino M, Meyer JH, Egers D (1989) Estimation of kappa number of pulps by near-infrared spectroscopy. *Tappi J* 72(9):193–197
- Bracewell R (1965) The Fourier transformation and its applications. McGraw-Hill, New York, 381 pp
- Cameron DG, Moffatt DJ (1984) Deconvolution, derivation, and smoothing of spectra using Fourier transforms. *Test Eval* 76:83
- Chang H-m, Sarkanen KV (1973) Species variation in lignins. Effect of species on the rate of kraft delignification. *Tappi* 56:132–134
- Chum HL, Ratcliff, Schroeder HA, Sopher DW (1984) Electrochemistry of biomass-derived materials. Characterization, fractionation, and reductive electrolysis of ethanol-extracted explosively depressurized aspen lignin. *J Wood Chem Technol* 4:505–532
- Compton DAC, Young JR, Kollar RG, Mooney JR, Grasselli JG (1987) In: McClure GL (ed) Computerized quantitative infrared analysis. ASTM, Philadelphia, 36–57
- Cooley JW, Tukey JW (1965) An algorithm for the machine calculation of complex Fourier series. *Math Comput* 19:297–301
- Faix O (1986) Investigations on lignin polymer models (DHP's) by FTIR spectroscopy. *Holzforschung* 40:273–280
- Faix O (1987) Quantitative FTIR-spektroskopische Untersuchungen an Ligninen und Ligninmodellsubstanzen. Habilitation Thesis, University of Hamburg
- Faix O (1991) Classification of lignins from different botanical origins by FTIR spectroscopy. *Holzforschung* 45 (Suppl, Sept):21–27
- Faix O, Beinhoff O (1988) FTIR spectra of milled wood lignins and lignin polymer models (DHPs) with enhanced resolution obtained by deconvolution. *J Wood Chem Technol* 8:505–522
- Faix O, Németh K (1988) Monitoring of wood photodegradation by DRIFT-spectroscopy. *Holz Roh- Werkst* 46:112
- Faix O, Patt R, Beinhoff O (1987) Grundlagen und Anwendung von FTIR-Spektroskopie bei der Herstellung und Analyse von Zellstoffen. *Papier* 41:657–663
- Faix O, Schweers W (1974) Vergleichende Untersuchungen an Polymermodellen des Lignins (DHPs) verschiedener Zusammensetzungen. 3 Mitt. IR-spektroskopische Untersuchungen. *Holzforschung* 28:50–54
- Ferraro JR, Basile LJ (1978) Fourier transform infrared: application to national problems. In: Ferraro JR, Basile LJ (eds) Fourier transform infrared spectroscopy – applications to chemical systems, Vol. 4. Academic Press, New York, 275–302
- Ferraro JR, Rein AJ (1985) Application of diffuse reflectance spectroscopy in the far-infrared region. In: Ferraro JR, Basile LJ (eds) Fourier transform infrared spectroscopy – applications to chemical systems, Vol. 4. Academic Press, New York, 244–282
- Frank IE, Feikema J, Constantine N, Kowalski BR (1984) Prediction of product quality from spectral data using the partial least squares method. *J Chem Inf Comput Sci* 24:20–24
- Fuller MP, Griffiths PR (1980) Infrared microsampling by diffuse reflectance Fourier transform spectrometry. *Appl Spectrosc* 34:533–539

- Gillette PC (1983) Factor analysis for separation of pure component spectra from mixture spectra. *Anal Chem* 55:630–633
- Gillette PC, Lando JB, Koenig JL (1985) A survey of infrared spectral data processing techniques. In: Ferraro JR, Basile LJ (eds) *Fourier transform infrared spectroscopy – applications to chemical systems*, Vol. 4. Academic Press, New York, 1–47
- Graham JA, Grim WM III, Fateley WG (1985) Fourier transform infrared photoacoustic spectroscopy of condensed-phase samples. In: Ferraro JR, Basile LJ (eds) *Fourier transform infrared spectroscopy – applications to chemical systems*, Vol. 4. Academic Press, New York, 345–392
- Grandmaison JL, Thibault J, Kaliaguine S, Chantal PD (1987) Fourier transform infrared spectrometry and thermogravimetry of partially converted lignocellulosic materials. *Anal Chem* 59:2153–2157
- Green DW, Reedy GT (1978) Matrix-isolation studies with Fourier transform infrared. In: Ferraro JR, Basile LJ (eds) *Fourier transform infrared spectroscopy – applications to chemical systems*, Vol. 1. Academic Press, New York, 1–59
- Griffiths PR (1975) *Chemical infrared Fourier transform spectroscopy*. Wiley, New York, 340 pp
- Griffiths PR (1983) Fourier transform infrared spectrometry. *Science* 222:297–302
- Griffiths PR, de Haseth JA (1986) *Fourier transform infrared spectrometry*. Wiley, New York, 672 pp
- Harbour JR, Hopper MA, Marchessault RH, Dobbin CJ, Anczurowski E (1985) Photoacoustic spectroscopy of cellulose, paper and wood. *J Pulp Pap Sci* 11:J42–J47
- Hauser M, Oelichmann J (1988) A critical comparison of solid sample preparation techniques in infrared spectroscopy. *Microchim Acta* (Wien), Spec. Issue, I:39–43
- Hergert HL (1971) Infrared spectra. In: Sarkanen KV, Ludwig CH (eds) *Lignins. Occurrence, formation, structure and reactions*. Wiley-Interscience, New York, 267–293
- Hirschfeld T (1987) In: McClure GL (ed) *Computerized quantitative infrared analysis*. ASTM, Philadelphia, 169–179
- Horlick G (1968) Introduction to Fourier transform spectroscopy. *Appl Spectrosc* 22:617–626
- Kawamura I, Higuchi T (1964a) Comparative studies of milled wood lignins from different taxonomical origins by infrared spectroscopy. In: *Grenoble Symposium 1964, Chimie et biochimie de la lignine, de la cellulose et des hemicelluloses*. Les Imprimeries Reunies de Chambéry, Chambéry, 439–456
- Kawamura I, Higuchi T (1964b) Studies on the properties of lignins of plants in various taxonomical positions II. On the I.R. absorption spectra of lignins. *Mokuzai Gakkaishi* 10:200–206
- Kawamura I, Shinoda Y, Nonomura S (1974) The comparison of relative intensities of IR absorption bands of MWL of various woods from tropical and temperate zones. *Mokuzai Gakkaishi* 20:15–20
- Kawamura I, Shinoda Y, Ai TV, Tanada T (1977) Chemical properties of lignin of Eyrthrina wood. *Mokuzai Gakkaishi* 23:400–404
- Koenig JL (1981) Fourier transform infrared spectroscopy of chemical systems. *Acc Chem Res* 15:171–178
- Krishnan K (1988) Characterization of semiconductor silicon using the FT-TR microsampling techniques. In: Messerschmidt RG, Harthcock MA (eds) *Infrared microspectroscopy: theory and applications*. Marcel Dekker, New York, 139–151
- Kuo MI, McClelland JF, Luo S, Chien PL, Walker RD, Hse CY (1988) Applications of infrared photoacoustic spectroscopy for wood samples. *Wood Fiber Sci* 20:132–145
- Lai Y-Z, Sarkanen KV (1975) Structural variation in dehydrogenation polymers of coniferyl alcohol. *Cellul Chem Technol* 9:239–245
- Mackenzie MW (1988) *Advances in applied Fourier transform infrared spectroscopy*. Wiley, New York, 350 pp
- Malhotra VM, Jasty S, Mu R (1989) FT-IR spectra of water in microporous KBr pellets and water's desorption kinetics. *Appl Spectrosc* 43:638–645
- Michell AJ (1988a) Note on a technique for obtaining infrared spectra of treated wood surfaces. *Wood Fiber Sci* 20:272–276

- Michell AJ (1988b) Infrared spectroscopy transformed – new applications in wood and pulping chemistry. *Appita* 41:375–380
- Michell AJ (1988c) Usefulness of Fourier-transform infrared difference spectroscopy for studying the reactions of wood during pulping. *Cellul Chem Technol* 22:105–113
- Michell AJ (1988d) Second derivative F.T.-I.R. spectra of celluloses I and II and related mono- and oligosaccharides. *Carbohydr Res* 173:185–195
- Michell AJ, Garland CP, Nelson PJ (1989) Diffuse-reflectance infrared Fourier transform (DRIFT) spectroscopic study of bleaching and yellowing of eucalypt cold soda pulp. *J Wood Chem Technol* 9:85–103
- Naes T, Martens H (1984) Multivariate calibration II. Chemometric methods. *Trends Anal Chem* 3:266–271
- Obst JR (1982) Guaiacyl and syringyl lignin composition in hardwood cell components. *Holzforschung* 36:143–152
- Obst JR, McMillan NJ, Blanchette RA, Christensen DJ, Crawford DM, Kuster TA, Landucci LL, Faix O, Newman RH, Pettersen RC, Schwandt VH, Weselowsky MF (1989) *Proc 5th Int Symp Wood Pulp Chem*, Raleigh, NC, Poster Sessions, 289–308, Tappi press, Atlanta, GA and Geological Survey of Canada, Bulletin 403 (1991):123–146
- Oelichmann J, Hauser M (1988) *Feststoffuntersuchungen in Infrarot-Spektroskopie*. Perkin Elmer's Applied Infrared Spectroscopy, 24, 7700 Überlingen, FRG
- Osborne BG, Fearn T (1986) Near infrared spectroscopy in food analysis. Langma Scientific and Wiley, New York, 200 pp
- Ostmeyer JG, Elder TJ, Winandy JE (1989) Spectroscopic analysis of southern pine treated with chromated copper arsenate II. Diffuse-reflectance Fourier-transform infrared spectroscopy (DRIFT). *J Wood Chem Technol* 9:105–122
- Owen NL, Thomas DW (1989) Infrared studies of “hard” and “soft” woods. *Appl Spectrosc* 43:451–455
- Painter P, Starsinic M, Coleman M (1985) Determination of functional groups in coal by Fourier transform interferometry. In: Ferraro JR, Basile LJ (eds) *Fourier transform infrared spectroscopy – applications to chemical systems*, Vol. 4. Academic Press, New York, 169–241
- Pakdel H, Grandmaison JL, Roy C (1989) Analysis of wood vacuum pyrolysis solid residues by diffuse reflectance infrared Fourier transform spectrometry. *Can J Chem* 67:310–314
- Perkins WD (1986) Fourier transform-infrared spectroscopy. Part I. Instrumentation. *J Chem Educ* 63:A5–A10
- Perkins WD (1987) Fourier transform-infrared spectroscopy. Part II. Advantages of FT-IR. *J Chem Educ* 64:A269–A271
- Rosencwaig A (1981) *Photoacoustics and photoacoustic spectroscopy*. Wiley, New York, 324 pp
- Salud EC, Faix O (1980) The isolation and characterization of lignins of *Shorea* species. *Holzforschung* 34:113–121
- Sarkanen KV, Chang H-m, Ericsson B (1967a) Species variation in lignins. Conifer lignins. *Tappi* 50:538–587
- Sarkanen KV, Chang H-m, Allan GG (1967b) Species variation in lignins. III. Hardwood lignins. *Tappi* 50:587–590
- Sarkanen KV, Hergert HL (1971) Classification and distribution. In: Sarkanen KV, Ludwig CH (eds) *Lignins. Occurrence, formation, structure and reactions*. Wiley-Interscience, New York, 43–94
- Sarkanen KV, Ludwig CH (1971) Definitions and nomenclature. In: Sarkanen KV, Ludwig CH (eds) *Lignins. Occurrence, formation, structure and reactions*. Wiley-Interscience, New York, 1–18
- Schiering DW, Oelichmann J, Rau A (1988) *Prinzipien und Anwendungen der Infrarot-Mikroskopie*. Perkin Elmer's Applied Infrared Spectroscopy, 7700 Überlingen, FRG
- Schultz TP, Templeton MC, McGinnis GD (1985a) Rapid determination of lignocellulose by diffuse reflectance Fourier transform infrared spectrometry. *Anal Chem* 57:2867–2869
- Schultz TP, McGinnis GD, Bertran MS (1985b) Estimation of cellulose crystallinity using Fourier transform-infrared spectroscopy dynamic thermogravimetry. *J Wood Chem Technol* 5:543–557

- Schultz TP, Glasser WG (1986) Quantitative structural analysis of lignin by diffuse reflectance Fourier transform infrared spectrometry. *Holzforschung* 40 (Suppl):37–44
- Schultz TP, Nicholas DD (1987) Fourier transform infrared spectrometry. Detection of incipient brown rot decay in wood. *Int Analyst* 41:35–39
- Sjöström M, Wold, S, Lindberg W, Persson J-A, Martens H (1983) A multivariate calibration problem in analytical chemistry solved by partial least-squares models in latent variables. *Anal Chim Acta* 150:61–70
- Sommer AJ, Lang PL, Miller BS, Katon JE (1988) Application of molecular microspectroscopy to paper chemistry. *Prac Spectrosc* 6 (Infrared Microspectrosc): 245–258
- Sweeney KM (1989) FTIR microscopy of pulp and paper samples. *Tappi J* 72(2):171–174
- Wetzel DL (1983) Near-infrared reflectance analysis. *Anal Chem* 55:1165A–1176A
- Williams P, Norris K (1987) Near-infrared technology in the agricultural and food industries. *Am Assoc of Cereal Chemists*, St. Paul, MN, 330pp
- Yang PW, Mantsch HH, Baudais F (1986) A critical evaluation of three types of diffuse reflectance infrared accessories. *Appl Spectrosc* 40:974–978
- Yasuda T, Sakakibara A (1981) Hydrogenolysis of protolignin in compression wood. V. Isolation of two trimeric compounds with lactone ring. *Holzforschung* 35:183–187
- Yeboah SA, Wang S-H, Griffiths PR (1984) Effect of pressure on diffuse reflectance infrared spectra of compressed powders. *Appl Spectrosc* 38:259–264
- Zavarin E, Nguyen C, Romero E (1982) Preparation of enzymatically liberated lignin from naturally brown-rotted wood. *J Wood Chem Technol* 2:343–37